

Hydrodynamic provinces and oceanic connectivity from a transport network help designing marine reserves

Vincent Rossi, Enrico Ser-Giacomi, Cristóbal López, and Emilio Hernández-García,¹
IFISC, Instituto de Física Interdisciplinar y Sistemas Complejos (CSIC-UIB). Campus
Universitat Illes Balears, Crta. Valldemossa km 7.5, E-07122 Palma de Mallorca,
Spain.

(Dated: July 28, 2014)

Oceanic dispersal and connectivity have been identified as crucial factors for structuring marine populations and designing Marine Protected Areas (MPAs). Focusing on larval dispersal by ocean currents, we propose an approach coupling Lagrangian transport and new tools from Network Theory to characterize marine connectivity in the Mediterranean basin. Larvae of different pelagic durations and seasons are modeled as passive tracers advected in a simulated oceanic surface flow from which a network of connected areas is constructed. Hydrodynamical provinces extracted from this network are delimited by frontiers which match multi-scale oceanographic features. By examining the repeated occurrence of such boundaries, we identify the spatial scales and geographic structures that would control larval dispersal across the entire seascape. Based on these hydrodynamical units, we study novel connectivity metrics for existing reserves. Our results are discussed in the context of ocean biogeography and MPAs design, having ecological and managerial implications.

I. INTRODUCTION

Oceanic ecosystems are impacted by multiple human-induced stressors, including habitat destruction, pollution, overfishing and global climate change. Marine protected areas (MPAs), used for the management and conservation of marine ecosystems, are considered effective to mitigate some of these impacts³⁶. Successful MPA design is however complicated primarily due to the difficulties in quantifying the movements of organisms, especially at larval stage⁵⁵, in resolving the multi-scale variability of ocean currents⁵⁶ and in apprehending the spatial scales and biogeography of the seascape²⁸.

Marine population connectivity, i.e. the exchange of individuals among geographically separated subpopulations, depends on numerous factors including spawning outputs, larval dispersal, habitat availability, trophic interactions and adult movements^{8,25}. Among them, larval dispersal has been identified as a crucial factor for structuring oceanic populations⁹ and for determining broad-scale ecological connectivity⁵⁹. It also plays a major role in assuring population persistence in a MPA network⁴³, especially when target species show long-distance dispersal⁵⁵. As such, patterns and magnitude of larval connectivity have been used to design MPAs³⁶ and assess their efficiency⁴⁹. This paper focuses on the dispersion of larvae by ocean currents at basin-scale, assuming they are passively transported by the flow (i.e. neglecting larval behavior), to inform the design of marine reserves.

Many biophysical modeling studies^{9,56}, includ-

ing Lagrangian approaches, examined marine connectivity from the so-called “connectivity matrix” which represents the probability of larval exchange between distant sites. Previous analyses were mainly limited to the strengths of pair-wise connections, i.e. the links from one coastal site, or MPA, to another distant one^{7,60}. Another perspective to investigate connectivity is the analysis of dispersal network topologies^{32,59}. Recent studies applied tools derived from Graph Theory to document regional connectivity of near-shore MPAs in the Baltic Sea⁴⁵, the Mediterranean Sea² and in the Great Barrier Reef region⁵⁷. While our understanding of connectivity at small- and regional-scales has improved, previous efforts focused mainly on coastal/insular areas and did not provide a characterization of the seascape connectivity.

The significance of this shortcoming is emphasized by the growing interests for the implementation of MPAs in the pelagic ocean^{26,48} which also shelters biodiversity and important ecological processes^{25,30}. Designing open-ocean MPAs is challenging partly because larval connectivity and pelagic habitats are difficult to assess in such vast and dynamic environment.

Here we use an approach coupling Lagrangian modeling and new tools from Network Theory⁴⁴ to characterize marine connectivity at basin-scale in the Mediterranean Sea. Larvae of different Pelagic Larval Durations (PLD) are modeled as passive Lagrangian particles advected in a simulated oceanic surface flow from which a network of connected areas can be constructed. Hydrodynamical provinces extracted from this transport

network are delimited by frontiers which match mesoscale and regional oceanographic features. We then identify the spatial scales and structures of larval dispersal across the entire seascape and analyse connectivity metrics for the existing Mediterranean MPAs. We finally discussed the usefulness of our results for the design of marine reserves and the characterization of oceanic biomes.

II. MATERIALS AND METHODS

A. Oceanic transport and connectivity from a Network Theory approach

The basic ingredients are (i) the tracking of passive Lagrangian particles (a model for larval transport) and (ii) the construction and analysis of a network of flow-mass transport. We study dispersal processes in the ocean based on a transport network in which:

- a *node* corresponds to a geographical sub-area of the oceanic surface,
- a *link*, or *edge*, symbolizes an effective mass transport driven by ocean currents between 2 sub-areas during a given time interval.

The transport network is thus composed of an ensemble of nodes (sub-areas), covering the entire oceanic domain of interest, which are interconnected by a number of links (transport pathways). Each link is *directed* in accord with the effective direction of the flow, and *weighted* proportionally to the amount of water flowing from one node to another. Many tools of Network Theory were designed to examine both local and global properties of such network⁴⁴, allowing us to explore geophysical flows and connectivity in a new fashion.

The Mediterranean Sea, a quasi-closed basin with its own physical circulation and ecological functioning under important human pressure¹², constitutes a natural laboratory for this study. In addition, it shelters already a hundred MPAs (whose locations were downloaded from the Med-Pan database) implemented for protection and conservation purposes. In this context, we aim at partitioning the surface Mediterranean seascape in hydrodynamical provinces, i.e. a set of oceanic subregions in which larvae/particles are much more likely to disperse efficiently within each other than among them at a given time-scale. This spatial subdivision in provinces is tantamount to detecting *communities* within the hydrodynamical network⁴⁴.

B. Lagrangian bio-physical modelling

The Lagrangian approach is a natural perspective to characterize transport phenomena affecting free-swimming larvae^{7,60}. Particles are advected in an eddy-resolving velocity field generated by the Nucleus for European Modeling of the Ocean hydrodynamical model implemented in the Mediterranean at a 1/16 *deg* horizontal resolution⁴⁶, (see also SI-text01). We focus on the upper-ocean dynamics over years 2002 – 2011 with the use of daily horizontal flow fields at 8 m depth (Fig. SI-1), representing the surface mixed layer in which larvae are assumed to be homogeneously distributed.

Horizontal trajectories are simulated by integrating the velocity field, bi-linearly interpolated at any sea point, using a *Runge-Kutta 4* algorithm with a time step of 1 day, matching the resolution of the simulated currents. Lagrangian particles are dispersed as two-dimensional passive drifters^{2,7}. Note that due to the non-fully incompressible horizontal flow field, vertical velocities may become significant in regions of strong divergence (e.g. coastal upwelling) and convergence (e.g. deep water formation). Neglecting vertical movements is however a reasonable assumption here because most particles remain in the selected layer over short time-scales (≤ 2 months) since horizontal velocities are several orders of magnitude higher than vertical ones¹⁷. Another simplification is the passive character of the particles, the implementation of more complex larval behavior (e.g. vertical migration, mortality, settlement) being envisaged for future work. Under these assumptions, larval dispersal is modulated by the PLD, the period of spawning and the time-varying oceanic circulation.

Initial (t_0) and integration ($\tau \sim \text{PLD}$) times are chosen according to the typical biological traits of marine organisms. Given the limited knowledge of their life cycles⁵⁵, we investigate basin-scale larval connectivity from an ecosystem-based approach^{4,26}, rather than focusing on a particular target species. To do so, we retain two different PLDs ($\tau = 30, 60$ days) and consider winter ($t_0 = 1^{\text{st}}$ Jan.) and summer ($t_0 = 1^{\text{st}}$ Jul.) spawning^{2,38,55} over the years 2002 – 2011. These modeling choices are ecologically meaningful for a number of Mediterranean organisms, especially those with wide geographical range and potential for large-distance dispersal (SI-text02). Sensitivity of our results to the parameter τ was tested by performing additional simulations for $\tau = 45$ days. A total of 60 factorial experiments (with starting times covering 2 seasons over 10 years, for each of the 3 PLDs) allow the construction of 60 connectivity matrices from which hydrodynamical

provinces are extracted (sect. III A). They are then temporally-averaged to describe robust spatial patterns of larval connectivity in the entire Mediterranean basin (sect. III B), finally interpreted in the context of MPA design (sect. III C).

C. Construction and analysis of a transport network

1. Connectivity matrix

The nodes of the transport network are defined by discretizing the surface ocean into 3270 quasi-square boxes of $1/4^\circ$ horizontal-resolution (Fig. SI-2), allowing the consideration of important mesoscale features of the Mediterranean circulation¹². This procedure and the numerical diffusion it introduces²² are detailed in SI-text01.

500 Lagrangian particles evenly distributed in each oceanic box are advected, corresponding to a total of ~ 1.6 millions trajectories in the Mediterranean basin for each experiment. The connectivity matrix is built using the initial and final positions of these particles. Each matricial element $\mathbf{P}_{ij}^{t_0, \tau}$, i.e. the link between nodes i and j , is proportional to the fraction of particles leaving box i at time t_0 and arriving in box j at time $t_0 + \tau$. $\mathbf{P}_{ij}^{t_0, \tau} = \# \text{ particles from box } i \text{ to box } j / N_i \in [0, 1]$ is interpreted as the probability for a particle selected randomly in box i at the initial time ending up in box j at the final time. N_i is a local normalization coefficient equal to the number of particles still within the oceanic domain after integration. Due to numerical limitations, some trajectories may indeed abort prematurely with the “beaching” of particles onto land areas. With this normalization, which concerns less than 5% of all particles for $\tau = 60$ days, the stochasticity of the matrix (i.e. its rows sum to 1) is ensured and the constraint of mass conservation fulfilled.

2. Community detection

To locate coherent regions in time-varying flows, the transport matrix approach has been proposed²². Such objects are extracted by examining eigenvalues⁴⁵ or singular vectors²⁴ of the transport (connectivity) matrix which approximates the continuous advection operator. These concepts, along with other community detection algorithms, were recently used to study ecological connectivity^{45,57}.

Here we analyze the topology of the transport network to subdivide the surface ocean in hydrodynamical provinces. Based on the connectivity

matrix $\mathbf{P}^{t_0, \tau}$, an equivalent of the network adjacency matrix, we detect communities using the *Infomap* algorithm⁵³. Random walkers are considered to move in the network according to the statistical description of the surface flow contained in the connectivity matrix. From these synthetic trajectories, and using information theory concepts, *Infomap* decomposes the network into a number of communities that define oceanic provinces well connected internally but with minimal exchanges of particle between them. The method is described and compared with other alternative in SI-text03.

To evaluate the significance of the spatial partitioning, we define a coherence ratio²⁴ associated with each province k by: $\rho_k = \sum_{i,j \in \mathcal{I}_k} N_i \mathbf{P}_{ij}^{t_0, \tau} / \sum_{i \in \mathcal{I}_k} N_i$ where \mathcal{I}_k is the set of indices that identify all boxes constituting province k . Physically, $\rho_k \in [0, 1]$ is interpreted as the fraction of particles initially released within a given province which remained in it after integration. Its complement $1 - \rho_k$ measures the proportion of particle leaking across the boundaries of each province.

III. RESULTS AND DISCUSSION

A. Time-dependent hydrodynamical provinces

The provinces and their boundaries are dynamical objects that evolve in space and time with different dimensions, shapes and locations (e.g. Fig. 1), due to the important variability of the ocean circulation⁴². The method captures an elevated number of communities in the network, with 65 provinces using a PLD = 30 days and only 32 for PLD = 60 days on the exemplary calculations displayed on Fig. 1. Intuitively, the longer the tracking time, the lower the number of provinces detected and the larger their mean area. On average over the ensemble of experiments, community detection results in 61, 46, 36 provinces characterized by a mean area of 4.12×10^4 , 5.5×10^4 , 6.8×10^4 (in km^2) for $\tau = 30, 45, 60$ days, respectively. Because of the time-varying flow⁵⁶, both release time and tracking duration (simulating respectively the initiation and duration of the pelagic larval phase) affect the spatial partitioning.

Most province boundaries match very well the mean flow streamlines (Fig. 1), suggesting high oceanographic relevance. While isolated streamlines are found in the cores of provinces, dense ones usually coincide with the detected boundaries. Hydrodynamical provinces are delimited by intense oceanic mesoscale structures such as jets, meanders, fronts and eddies. These features, which influence the topology of the transport network

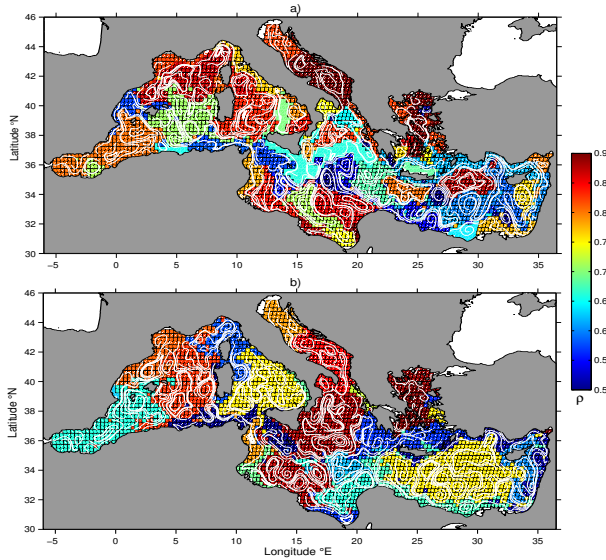


Figure 1. Hydrodynamical provinces extracted from the connectivity matrices of a) Winter 2011 ($t_0 = 1^{st}$ Jan.) using $\tau \simeq PLD = 30$ days and b) Summer 2011 ($t_0 = 1^{st}$ Jul.) using $\tau \simeq PLD = 60$ days. Each province is colored according to its ρ value (ranging from 0.5 to 0.9). White streamlines represent the simulated flow averaged over the period of integration (i.e. a) 1^{st} - 30^{th} Jan. 2011 and b) 1^{st} Jul.- 29^{th} Aug. 2011).

and thus the community detection, were recently reported to strongly impact connectivity⁶⁰. For instance, some mesoscale eddies are extracted as quasi-circular single provinces (e.g. in the Alboran Sea and in the southern Levantine basin), in good agreement with the flow streamlines (Fig. 1a). Other mesoscale structures are contained in larger provinces. The method allows the optimal detection of coherent oceanic sub-regions originating from the ocean circulation and its multiscale variability.

The coherence ratios are generally elevated ($\rho \in [0.5, 1]$) and variable (Fig. 1). Although it depends on both the local leaking processes and the area of a given province, there is no apparent relationship between the size of the sub-region and its coherence ratio. Overall, $\rho \geq 0.8$ are often seen in the Aegean and Adriatic Seas. The Alboran, Balearic, Tyrrhenian, and Adriatic Seas are characterized by relatively large provinces, whereas the Levantine, Aegean and south Ionian and Libyan Seas are subdivided in rather small ones. Note also that some provinces are composed of non-contiguous boxes. This occurs especially within the pathways of fast-flowing currents as the Algerian Current, the Atlantic-Ionian stream (south Ionian, Libyan and south-east Levantine sea) and

the Liguro-Provençal Current (Ligurian sector).

B. Spatial-scales and geographic structure of larval dispersal

The frequency of occurrence of province boundaries is now examined across the ensemble of experiments to identify recurrent frontal systems and relatively stable hydrodynamical units which would organise larval dispersal. Over most coastal/shallow regions, boundaries occur in various locations and orientations, resulting in no apparent structure (dark red patches). These disorganized patterns characterize oceanic environments with complex circulation in which spatial-scales of connectivity are highly variable⁵⁶. They are observed in most insular regions (Balearic, Tuscan and Aegean archipelagos, Corsica, Sardinia, Crete, Cyprus), in the Tunisian-Sicilian strait (also punctuated by small islands) and over narrow continental shelves (Italian, French, Catalan, Libyan-Egyptian and Israelian-Lebanon shelves) (Fig. 2a). In contrast, wide continental shelves are organized as coherent hydrodynamical units whose offshore limits match the 200 m isobath. The gulf of Lion is delimited by a frontier coinciding with the Catalan front and associated Northern current³ (an extension of the Liguro-Provençal current). For long PLDs only, the Tunisian-Libyan shelf appears as two units in summer (Fig. 2b), merging into a single one in winter. The oceanic frontiers constituted by such currents/fronts are likely to prevent coastal larvae from escaping wide continental shelves.

In the open ocean, clear hydrodynamical units emerge (Fig. 2), organized as large “gyre” systems with rare occurrence of boundaries (white/yellow colors) in their center and semi-persistent frontiers (light/dark red colors) aligned along their perimeters. Elevated connectivity within each subdivision but little exchange between them are expected, thus providing basin-scale patterns of larval dispersal. Large hydrodynamical units are found in the western Mediterranean basin, the Adriatic sea, the Tyrrhenian sea (Fig. 2a and b) and only at longer time-scales in the north-Ionian and Levantine seas (Fig. 2b). Most of these open-ocean frontiers are located along well-known oceanographic features⁴², some of them recognized as partial transport barriers. For instance, the so-called Oran-Almeria front separates the Alboran sea from the rest of the Mediterranean Sea. It appears here rather extending from Oran to Cartagena, some 200 km away than previously documented¹². The Balearic front is another semi-permanent transport barrier⁴⁰ passing north of

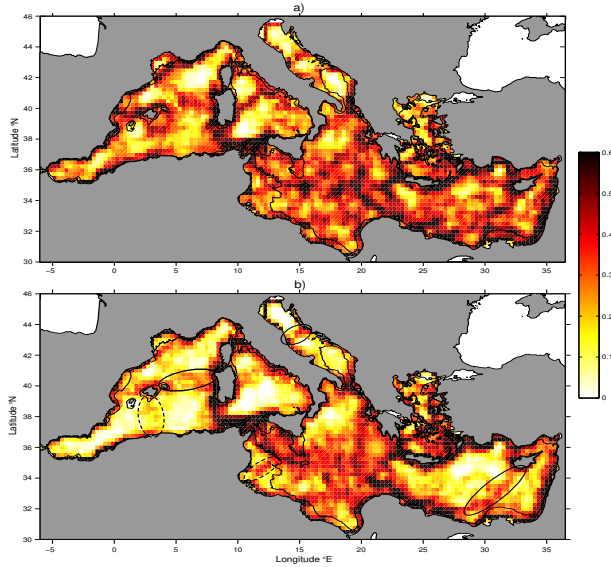


Figure 2. Frequency of occurrence of province boundaries at each ocean node from the ensemble of 20 experiments (all winters/summers of 2002 – 2011) for each PLD: a) $\tau \simeq PLD = 30$ days and b) $\tau \simeq PLD = 60$ days. Black ellipses in b) highlight the frontiers which have significant seasonality: plain ellipses indicate a preferential occurrence in winter and dotted ellipses in summer. Black contours represent the 200 m isobath.

the Balearic archipelago in the Balearic current³ and elongating eastward in winter. North of this quasi-zonal boundary, a large hydrodynamical unit composed of the Lion gyre and Ligurian sea is separated from the Balearic sea at short time-scale. The Tyrrhenian sea is consistently organized as a two-gyre system using both PLDs. For the 30-day integration the Adriatic sea is subdivided by bathymetric gradients (~ 100 and 200 m isobaths, i.e. off the Gargano promontory) into a northern, central and southern Adriatic gyres, the two latter units merging for PLDs of 60 days.

Surprisingly, some open-ocean areas, such as the Ionian, Levantine and Aegean basins (Fig. 2a), are characterized by disorganized dispersal patterns and stochastic larval connectivity⁵⁶. They become more structured at longer time-scales with the emergence of the Western Ionian gyre, the Shikmona gyre and a large system encompassing the Rhodes, Ierapetra and Mersa-Matruh gyres⁴². The eastern Aegean sea has disorganized dispersal patterns whereas small hydrodynamical units appear in its northern and western parts, in good agreement with its thermal structure⁵².

More generally, regions with no apparent spatial patterns at short PLDs see the emergence of spatial structures for longer integration time. Oceanic

areas already identified as gyral systems for short time-scales have their diameter increasing with the integration time, ultimately merging with their neighbors.

Note that most of these hydrodynamical units are quite consistent with the trophic clusters obtained from satellite chlorophyll data¹⁶, suggesting they also delimits specific biogeochemical provinces³⁷. Indeed, although this study focuses on passive larvae, the unveiling of well-known oceanic fronts and gyres hint that the spatial distribution of other tracers (e.g. salinity, temperature, chlorophyll-*a*, dissolved nutrients) are also influenced by similar transport patterns.

C. Implications for the design of marine reserves

The geographical structure of larval dispersal in the seascape influences largely the connectivity of marine reserves. The MPAs located within large and stable hydrodynamical units (Fig. 2) are interconnected, in good agreement with² who identified similar MPA clusters in the Algerian, Balearic, Adriatic and Tyrrhenian seas, respectively. Further information is obtained with the analysis of three complementary proxies of connectivity defined as followed. We analyze the mean spatial scales of larval dispersal (Fig. 3a) and the mean local coherence (inversely related to leaking, Fig. 3b) by averaging over the ensemble of experiments the area and the coherence ρ , respectively, of the time-dependent province encompassing each MPA. While these two metrics are solely influenced by the flow, the mean number of interconnected MPAs (i.e. temporally averaged number of MPAs encountered within the same time-dependent province, Fig. 3c) depends also on the density of existing reserves.

Larval connectivity and dispersal potentials are highly variable among the Mediterranean MPAs (Fig. 3). Reserves in the Adriatic and Aegean seas are characterized by small dispersal surface ($\leq 5 \times 10^4 \text{ km}^2$) and among the highest coherence ($\rho \geq 0.8$). This suggests a low connectivity which is also reflected in the few interconnected MPAs (≤ 8) despite their relatively high density. MPAs located around isolated islands are associated with modest dispersal surface ($\sim 4\text{--}8 \times 10^4 \text{ km}^2$) and low coherence ($\rho \leq 0.7$). Typical of these insular environments⁶⁰, complex circulation patterns (islands' wake, eddies, retention...) result in a moderate connectivity and high temporal variability (not shown). MPAs implemented within narrow continental shelves bounded by energetic currents are characterized by rather large provinces ($\geq 7 \times 10^4 \text{ km}^2$) and moderate coher-

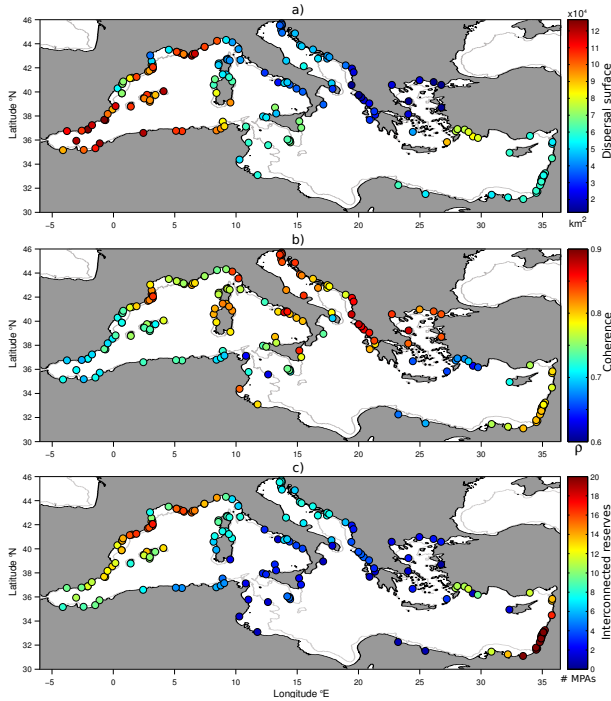


Figure 3. Spatial variability of MPAs connectivity derived from three complementary metrics averaged over all winter/summer experiments over 2002 – 2011 using $\tau \simeq PLD = 30$ days. a) Mean area (in km^2) and b) mean ρ of the province sheltering the reserve of interest. c) Mean number of interconnected MPAs (i.e. number of reserves situated within the same hydrodynamical province). Light grey contours represent the 200 m isobath. Results using a PLD of 45 and 60 days are qualitatively similar with a slight increase of the mean area and the number of interconnected reserves. Note that non-contiguous areas belonging administratively to a given reserve were treated here as a single MPA.

ence ($0.65 \leq \rho \leq 0.8$). These reserves are situated along the French Côte d’Azur with the Liguro-Provençal Current, the Catalan coast with the Northern Current, the Moroccan/Algerian coastlines impacted by the Algerian Current and in the eastern Levantine basin with the jet-like intensifications of its gyre circulation⁴². This elevated connectivity is driven by the adjacent currents that regularly intrude onto the shelf, enhancing larval dispersal along the current axis, as suggested by the numerous interconnected MPAs (≥ 15) along the French, Catalan and Israeli coastlines. In contrast, MPAs situated within extended continental shelves, such as the Gulf of Lion and the Tunisian/Libyan shelf, are characterized by small dispersal area ($\leq 6 \times 10^4 km^2$) and large coherence ($\rho \geq 0.8$). Unless exceptional intrusion events

(not shown), the inner-shelf is isolated by shallow bathymetry holding the current off the shelf break, thus resulting in restricted connectivity. Note that most MPAs associated with narrow shelves and sluggish circulation (such as the Tyrrhenian, Corsican and Sardinian coastlines) behave quite similarly to the latter group with small dispersal surfaces.

Despite the stochastic nature of larval dispersal⁵⁶, local oceanographic characteristics result in the emergence of connectivity regimes. They should be in accord with the main conservation objectives to ensure successful implementations of coastal and offshore marine reserves. For instance, the allocation of MPAs within narrow shelves bounded by currents would favor larval export over large distances⁴⁹ whereas reserves created within internal seas or large continental shelves would rather promote the restoration of local populations⁵⁰. Overall, the Mediterranean MPAs are not evenly distributed across the spatial partitioning of the seascape revealed by our analysis (sect. IIIB)¹¹. Moreover, the “size and spacing” guidelines already studied theoretically⁴³, may differ depending on the local dispersal behavior. Our results suggest the use of few large MPAs located in each stable hydrodynamical unit of the western Mediterranean basin and the Adriatic sea whereas numerous small MPAs evenly distributed across the fluctuating units might be preferable in the Ionian and Aegean seas.

IV. GENERAL CONCLUSIONS AND PERSPECTIVES

Using a method coupling Lagrangian trajectories and new tools from Network Theory, we study larval dispersal by surface currents in the Mediterranean Sea. Under our assumptions, a transport network is constructed from the horizontal advection of passive particles in a modelled oceanic flow, simulating larvae of different planktonic seasons and durations. The systematic detection of communities in the network extracts a set of hydrodynamical provinces which organize the surface dispersion of larvae in the entire Mediterranean basin. Their boundaries coincide with both mesoscale and regional-scale oceanographic features, comprehending the multiscale processes of ocean circulation. The repeated occurrence of these frontiers allows separating the seascape in different hydrodynamical units which provide the “backbone” of oceanic transport impacting larval dispersal and connectivity among existing MPAs. While the role of such large-scale dispersal patterns on the ge-

netic structure of marine population remain to be determined, the hydrodynamical units evidenced may be used to optimize the sampling strategy of genetic studies. The similarity between our flow-driven boundaries and major environmental gradients commonly used to regionalize the Mediterranean seascape finally suggests they might also define oceanic biomes or even faunistic units. Future developments of the methodology would have to consider more realistic larval behavior for a given target species as well as full tridimensionality of the flow. These extensions may help incorporating large-scale biogeography and dispersal patterns to improve MPAs design toward efficient management and conservation of marine ecosystems.

ACKNOWLEDGMENTS

The authors acknowledge support from MICINN and FEDER through the ESCOLA project (CTM2012-39025-C02-01) and support from ECs Marie-Curie ITN program (FP7-PEOPLE-2011-ITN) through the LINC project (no. 289447). The simulated velocity field used in this study was generated by MyOcean (<http://www.myocean.eu/>) and the locations of Mediterranean MPAs were provided by MedPan (<http://www.medpan.org/>). The authors thank the two anonymous reviewers who helped improving the original manuscript.

V. SUPPLEMENTARY INFORMATION 1: EDDY-RESOLVING MODEL AND DISCRETIZATION PROCEDURE

A. Hydrodynamical model of the Mediterranean Sea

The Mediterranean Forecasting System is a hydrodynamic model based on NEMO-OPA (Nucleus for European Modelling of the Ocean-PARallelisé, version 3.2³⁹) with a variational data assimilation scheme. It is a primitive equations model in spherical coordinates, implemented in the Mediterranean at $\frac{1}{16}$ deg horizontal resolution and 72 unevenly spaced vertical levels⁴⁶. We use here the "Physics reanalysis" component for years 2002–2011 downloaded from MyOcean website.

The model covers entirely the Mediterranean Basin and extends into the Atlantic in order to better resolve the exchanges with the Atlantic Ocean at the Strait of Gibraltar. It is nested, in the Atlantic, within the monthly mean climatological fields computed from ten years of daily output of the $\frac{1}{4}$ deg global model¹⁸. Details on the nesting technique and major impacts on the model results can be found elsewhere⁴⁶. The model uses vertical partial cells to fit the bottom depth shape. It is forced by momentum, water and heat fluxes interactively computed by bulk formula using the 6-h, 0.25 deg horizontal-resolution operational analysis and forecast fields from the European Centre for Medium-Range Weather Forecasts. Air-sea processes predict surface temperature⁵⁸, while the water balance is computed as Evaporation minus Precipitation and Runoff. The evaporation is derived from the latent heat flux; the precipitation and the runoff are provided by monthly mean datasets. The Dardanelles inflow is parameterized as a river using climatological net inflow rates³³.

The data assimilation system is the OCEAN-VAR scheme¹⁵. The background error correlation matrices, estimated from the temporal variability of parameters in a historical model simulation, vary seasonally in the sub-regions of the Mediterranean Sea characterized by different physical characteristics¹⁴. The Mean Dynamic Topography is used for the assimilation of Sea Level Anomaly (SLA)¹³. The assimilated data include: along track SLA, satellite Sea Surface Temperature (SST), in-situ temperature profiles by eXpandable Bathymetry Thermograph, in-situ temperature and salinity profiles by Argo floats, in-situ temperature and salinity profiles from Conductivity-Temperature-Depth casts. Objective Analyses of SST data are used for the correction of surface heat fluxes with the relaxation constant of $40 \text{ W m}^{-2} \text{ K}^{-1}$.

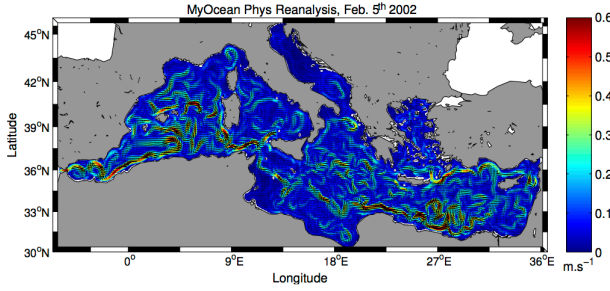


Figure 4. Snapshot of the surface (8 m) velocity field for February 5th 2002. Background colors represent the modulus ($m s^{-1}$) of the instantaneous velocity field which is superimposed as black vectors (note that the original $1/16$ deg resolution of the vector field has been coarse-grained for visualization purposes).

An exemplary snapshot of the surface (8 m) velocity field generated by this configuration and used to integrate Lagrangian particle trajectories is displayed in Fig. SI-4. Note the realistic representation of both large- and small-scale oceanographic features.

B. Discretization procedure to define the network nodes

The nodes of the transport network are delineated by discretizing the continuous ocean into quasi-square boxes of $1/4$ deg horizontal-resolution, of the order of important mesoscale features of the Mediterranean circulation^{12,42}. The ocean surface is subdivided into a total of 3270 two-dimensional boxes, imposing equal-area (~ 772 km²) with the use of a sinusoidal projection (see Fig. SI-5). This procedure introduces numerical diffusion below the scales of discretization²² so that sub-mesoscale dynamics are not explicitly resolved.

The simulated currents used to compute the Lagrangian trajectories (e.g. Fig. SI-4) contain smaller scale structures since they were generated at $1/16$ deg, i.e. 6-8 km at these latitudes. The box length-scale of $1/4$ deg intervene in the community detection algorithm (so that the numerical diffusion introduced is impacting the spatial precision of their boundaries).

Adding noise (or random walk) to the Lagrangian trajectories to represent non-resolved small-scale processes is not necessary here, as our discretization procedure already introduces an implicit diffusion. It can be estimated by considering that, away from strong fronts, the currents in the surface ocean are incompressible and two-

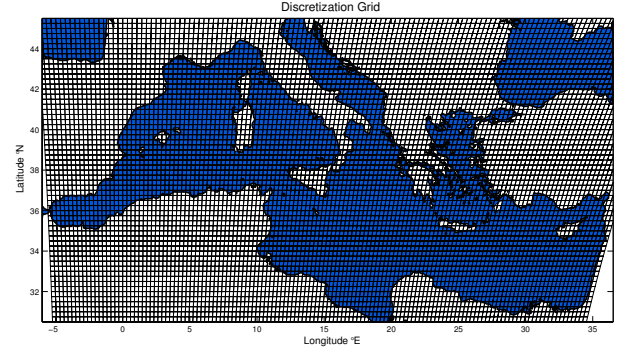


Figure 5. Discretization grid used to construct the transport network. Each quasi-square box of $1/4$ deg horizontal-resolution represents a node of the network.

dimensional, so that locally the flow is dominated by strain. Under the influence of this flow, patches of tracer (i.e. larvae, chlorophyll-*a*, etc...) evolve towards filamental structures^{1,41} of typical width $L = \sqrt{D/\lambda}$, where D is the diffusivity coefficient and λ the rate of strain (or Lyapunov exponent) of the flow. From this expression, one can estimate an effective diffusion coefficient $D = \lambda L^2$, associated to structures resolved by our discretization of size L . Since λ spans $0.01 - 0.1$ day⁻¹ in the Mediterranean Sea¹⁷ and $L = 1/4$ deg (~ 25 km at these latitudes), this formula gives a numerical diffusivity $O(1 - 10^2)$ m²s⁻¹.

Other estimations, e.g. based on Okubo's formula associated to a given resolution of the velocity field^{29,47} provide values for the diffusivity of the same order of magnitude. Indeed eddy diffusivity coefficients in the Mediterranean Sea range from 1 to 100 m²s⁻¹, while a value of 10 m².s⁻¹ has been used in Lagrangian tracking model⁵⁴, falling precisely within the range of our estimations. This is also similar to the random noise typically added to Lagrangian trajectories. For instance a diffusion of 0.2 m²s⁻¹ was used with a fine-scale numerical model at ~ 4 km spatial resolution⁶⁰, implying higher values (that would be within our estimated range) for a coarser model like the one we used. According to these estimates, the artificial diffusion introduced by our method is, in all cases, similar or even higher than the random noise typically added to Lagrangian trajectories to simulate unresolved sub-grid processes.

VI. SUPPLEMENTARY INFORMATION 2: ECOLOGICAL RELEVANCE OF OUR NUMERICAL EXPERIMENTS

The need for an ecosystem-based management of marine resources has been emerging^{31,51}, especially in the Mediterranean basin^{4,5,26}. For instance, recent studies considered an ecosystem-based approach to optimize the location of reserves for several species based on multi-factorial analysis³⁴ or to inform MPA efficiency by modelling trophic interactions within the whole ecosystem⁶. In the context of assessing larval connectivity for MPAs design, it implies the need of considering the ecosystem as a whole rather than focusing on a specific organism²⁷. This is implemented here by simulating a range of different PLDs and periods of spawning which are, under certain assumptions, biologically relevant for a number of Mediterranean species.

A compilation of the mean Pelagic Larval Durations (PLDs) of 62 littoral Mediterranean fishes revealed they span 10-70 days depending on the species considered, with large intra-species variability³⁸. Considering the "basin-scale" angle of our study, we focus on species with a wide geographical range and potential for large-distance dispersal. These organisms are usually characterized by pelagic spawning, long PLDs (≥ 20 days) and offshore larval distribution (although many combinations of such early life traits exist)³⁸. We retain a PLD of 30 days which is the best estimate available for a few iconic species of the Mediterranean ecosystem, including some demersal fishes (e.g. the groper *Epinephelus marginatus*², the blenny *Lipophrys canevai*, the wrasse *Labrus viridis*, the goatfish *Mullus surmuletus*, the bream *Sarpa salpa*³⁸) and invertebrates (e.g. the crab *Pachygrapsus marmoratus*²¹). We also performed simulations for a PLD of 60 days since other Mediterranean fishes (e.g. the blenny *Lipophrys trigloides*³⁸) and most marine invertebrates (echinoderms like the sea-star *Astropecten aranciaceus*⁶¹, some molluscs and many exploited crustaceans⁵⁵) are characterized by long PLD.

Dispersal potential can also be influenced by other mechanisms than PLD, such as early life traits. However, because the precise description of spawning strategy and larval distribution of marine organisms remains elusive, a classification was proposed based on its preferential season and location of occurrence³⁸. A large majority of the species they studied (e.g. *Epinephelus marginatus*, *Lipophrys canevai*, *Mullus surmuletus*) spawn in late spring / early summer, so we assume that summer is the season of their planktonic life. Some others (e.g. *Sarpa salpa*, *Lipophrys trigloides*) prefer a

late autumn / early winter spawning, resulting in the highest abundance of larvae observed in winter. Concerning spatial preferences, the "coastal spawners" (e.g. *Labrus viridis*) release their eggs close to the bottom in shallow areas and then their planktonic larvae are concentrated in the coastal ocean. In contrast, the "pelagic spawners" (e.g. *Epinephelus marginatus*, *Mullus surmuletus*, *Sarpa salpa*) spawn in the open-ocean with their larvae found widespread offshore³⁸.

To sum-up, an ensemble of Lagrangian simulations covering both coastal and open-ocean regions were carried-out for each PLD over all years 2002 – 2011 with two starting dates, a winter ($t_0 = 1^{st}$ Jan.) and a summer ($t_0 = 1^{st}$ Jul.) calculations. Our basin-scale patterns of connectivity (Fig. 2 and 3) are extracted from the temporally-averaged hydrodynamical provinces (thus erasing the impact of the inter-annual variability of the circulation), i.e. derived from more than 30 millions trajectories per PLD. It leads to statistically robust and ecologically meaningful patterns of larval connectivity in the Mediterranean basin, providing useful results in the context of an ecosystem-based MPA design.

VII. SUPPLEMENTARY INFORMATION 3: THE INFOMAP COMMUNITY DETECTION METHOD

A. Why using Infomap?

Once the transport problem is cast in terms of network concepts by constructing the connectivity matrix $\mathbf{P}^{t_0, \tau}$, a variety of mathematical tools becomes available for the question of dividing the sea into well-connected regions called “communities” in the network theory parlance^{10,19,35,44}. Among the numerous methods available, we choose *Infomap*⁵³, a well known algorithm in the Network community, to identify community structure in our hydrodynamic networks. It retains both the “direction” and “weight” information of each link by mapping the system-wide flow induced by local interactions between nodes. This is a key feature of the method since the weights (amount of water transported) and directions (of the flow) in our transport network are crucial to represent the true oceanic circulation.

This flow-based approach is indeed necessary to identify the most important structural aspects of networks where links represent patterns of movement among nodes (such as the transport network built here). In contrast, other topological methods which also use “direction” and “weight” (i.e. modularity optimization or cluster-based compression) are well adapted to analyse networks whose links do not represent flows but rather pairwise relationships, since they are blind to interdependence in flow networks⁵³. In addition, *Infomap* does not require to specify *a priori* the number of communities to be detected. It finds structures which are directly related to well-mixed regions under the flow represented by $\mathbf{P}^{t_0, \tau}$, and not to other structural properties (for example, a well defined region with strong fluxes oriented towards a particular direction) which will not lead to particle localization in that region. Also, *Infomap* does not assume communities with similar sizes (as for example the spectral partitioning²³) nor suffers from the “resolution limit”²⁰ which limits the minimum community size detectable by most algorithms. In fact, the transport network is decomposed into pieces of different sizes in regions where the flow requires so (e.g. Fig. 1).

All these properties make it very suitable for our purpose of identifying well mixed oceanic regions which are relatively less connected with the surroundings. Last but not least, the minimization algorithm is computationally efficient, well documented and publicly available (<http://www.tp.umu.se/~rosvall/code.html>).

B. How it works?

Infomap considers an ensemble of random walkers in the network characterized by $\mathbf{P}^{t_0, \tau}$, moving with the transition probabilities in that matrix. Then, the method addresses from the information-theory point of view the question of optimally coding the ensemble of possible random walks. To this end the network is divided in communities and each random walk is coded by sequences of words that represent successive locations inside a community and jumps to a different community. The information-theoretic lower bound to the average length of the codeword used is given in terms of the transition probabilities and of the specific partition in communities by the so-called *map equation*. For a network characterized by a directed and weighted adjacency matrix, equivalent to our connectivity matrix $\mathbf{P}^{t_0, \tau}$, this map equation is:

$$L = q_{\curvearrowright} H(\mathcal{Q}) + \sum_{\alpha=1}^c p_{\mathcal{Q}}^{\alpha} H(\mathcal{P}^{\alpha}) . \quad (1)$$

c is the number of communities in the particular partition considered. The first term involves the Shanon entropy associated to the transitions between different communities α :

$$H(\mathcal{Q}) = - \sum_{\alpha=1}^c \frac{q_{\alpha\curvearrowright}}{q_{\curvearrowright}} \log_2 \left(\frac{q_{\alpha\curvearrowright}}{q_{\curvearrowright}} \right) \quad (2)$$

$q_{\alpha\curvearrowright}$ is the probability to leave community α in one random-walk step, and $q_{\curvearrowright} = \sum_{\alpha=1}^c q_{\alpha\curvearrowright}$. Expressions for these quantities in terms of the components of the network matrix $\mathbf{P}^{t_0, \tau}$ exist⁵³. The second term in Eq. (1) contains the Shanon entropies $H(\mathcal{P}^{\alpha})$ associated to the words used to codify the position inside a community α and the word that denote the exit from that community:

$$H(\mathcal{P}^{\alpha}) = - \sum_{i \in \alpha} \frac{\pi_i}{p_{\mathcal{Q}}^{\alpha}} \log_2 \left(\frac{\pi_i}{p_{\mathcal{Q}}^{\alpha}} \right) - \frac{q_{\alpha\curvearrowright}}{p_{\mathcal{Q}}^{\alpha}} \log_2 \left(\frac{q_{\alpha\curvearrowright}}{p_{\mathcal{Q}}^{\alpha}} \right) . \quad (3)$$

The notation $i \in \alpha$ indicates sum over the nodes pertaining to community α . π_i is the stationary distribution of the random walk and $p_{\mathcal{Q}}^{\alpha} = q_{\alpha\curvearrowright} + \sum_{i \in \alpha} \pi_i$. Again, expressions for these quantities can be obtained from the elements in the network matrix $\mathbf{P}^{t_0, \tau}$ ⁵³.

Infomap finds the partition that minimizes the quantity in (1), i.e. the partition that provides a shorter description of the ensemble of walks going in and outside the communities. In other words, it finds the partition for which the random walks

remain most of the time inside the communities with few jumps between them. This minimization process uses a deterministic Greedy algorithm followed by a simulated-annealing algorithm which was repeated 100 times to select the best partition in provinces (although the results were already stable after 10 attempts).

REFERENCES

- ¹Abraham, E., C. Law, P. Boyd, S. Lavender, M. T. Maldonado, and A. Bowie (2000), Importance of stirring in the development of an iron-fertilized phytoplankton bloom, *Nature*, *407*, 727–730.
- ²Andrello, M., D. Mouillot, J. Beuvier, C. Albouy, W. Thuiller, and S. Manel (2013), Low connectivity between mediterranean marine protected areas: A biophysical modeling approach for the dusky grouper *Epinephelus marginatus*, *Plos 1*, *8*(7), e68,564.
- ³Bouffard, J., A. Pascual, S. Ruiz, Y. Faugère, and J. Tinotore (2010), Coastal and mesoscale dynamics characterization using altimetry and gliders: A case study in the Balearic sea, *J. Geophys. Res.*, *115*, C10,029.
- ⁴Coll, M., et al. (2012), The Mediterranean Sea under siege: spatial overlap between marine biodiversity, cumulative threats and marine reserves, *Global Ecol. Biogeogr.*, *21*, 465–480.
- ⁵Coll, M., et al. (2013), The scientific strategy needed to promote a regional ecosystem-based approach to fisheries in the Mediterranean and Black Seas, *Rev. Fish Biol. Fisheries*, *23*, 415–434.
- ⁶Colleter, M., D. Gascuel, J.-M. Ecoutin, and L. T. de Morais (2012), Modelling trophic flows in ecosystems to assess the efficiency of marine protected areas: a case study on the coast of Senegal, *Ecol. Model.*, *232*, 1–13.
- ⁷Corell, H., P.-O. Moksnes, A. Engqvist, K. Doos, and P. Jonsson (2012), Depth distribution of larvae critically affects their dispersal and the efficiency of marine protected areas, *Mar. Ecol. Prog. Ser.*, *467*, 29–46.
- ⁸Cowen, R. K., and S. Sponaugle (2009), Larval dispersal and marine population connectivity, *Annu. Rev. Mar. Sci.*, *1*, 433–466.
- ⁹Cowen, R. K., C. B. Paris, and A. Srinivasan (2006), Scaling of connectivity in marine populations, *Science*, *311*, 522–527.
- ¹⁰Danon, L., A. Díaz-Guilera, J. Duch, and A. Arenas (2005), Comparing community structure identification, *J. Stat. Mech.*, *09*, P09,008.
- ¹¹De-Juan, S., et al. (2012), A regional network of sustainable managed areas as the way forward for the implementation of an Ecosystem-Based Fisheries Management in the Mediterranean, *Ocean Coast. Manage.*, *65*, 51–58.
- ¹²de Madron, X. D., et al. (2011), Marine ecosystems' responses to climatic and anthropogenic forcings in the mediterranean, *Prog. Oceanogr.*, *91*, 97–166.
- ¹³Dobricic, S. (2005), New mean dynamic topography of the Mediterranean calculated from assimilation system diagnostic, *Geophys. Res. Lett.*, *32*(11), L11,606.
- ¹⁴Dobricic, S., N. Pinardi, M. Adani, M. Tonani, C. Fratianni, A. Bonazzi, and V. Fernandez (2007), Daily oceanographic analyses by Mediterranean Forecasting System at the basin scale, *Ocean Sci.*, *3*, 149–157.
- ¹⁵Dobricic, S., and N. Pinardi (2008), An oceanographic three-dimensional variational data assimilation scheme, *Ocean Model.*, *22*(3–4), 89–105.
- ¹⁶d'Ortenzio, F., and M. R. d'Alcalá (2009), On the trophic regimes of the Mediterranean sea: a satellite analysis, *Biogeosc.*, *6*, 1–10.
- ¹⁷d'Ovidio, F., V. Fernandez, E. Hernandez-García, and C. Lopez (2004), Mixing structures in the mediterranean sea from Finite-Size Lyapunov Exponents, *Geophys. Res. Lett.*, *31*, L17,203.
- ¹⁸Drévilion, M., et al. (2008), The GODAE/Mercator ocean global ocean forecasting system: results, applications and prospects, *J. Operational Ocean.*, *1*, 51–57.
- ¹⁹Fortunato, S. (2010), Community detection in graphs, *Phys. Rep.*, *486*, 75–174.
- ²⁰Fortunato, S., and M. Barthélemy (2007), Resolution limit in community detection, *P. Natl. Acad. Sci. USA*, *104*, 36–41.
- ²¹Fratini, S., L. Ragionieri, G. Cutuli, M. Vannini, and S. Cannicci (2013), Pattern of genetic isolation in the crab *Pachygrapsus marmoratus* within the Tuscan archipelago (Mediterranean sea), *Mar. Ecol. Prog. Ser.*, *478*, 173–183.
- ²²Froyland, G., and M. Dellnitz (2003), Detecting and locating near-optimal almost-invariant sets and cycles, *SIAM J. Sci. Comput.*, *24*(6), 1839–1863.
- ²³Froyland, G., K. Padberg, M. H. England, and A.-M. Treguier (2007), Detection of coherent oceanic structures via transfer operators, *Phys. Rev. Lett.*, *98*, 224,503.
- ²⁴Froyland, G., C. Horenkamp, V. Rossi, N. Santitisadeekorn, and A. S. Gupta (2012), Three-dimensional characterization and tracking of an Agulhas ring, *Ocean Model.*, *52*, 69–75.
- ²⁵Game, E. T., et al. (2009), Pelagic protected areas: the missing dimension in ocean conservation., *Trends Ecol. Evol.*, *24*(7), 360–369.
- ²⁶Guidetti, P., G. Notarbartolo-Di-Sciara, and T. Agardy (2013), Integrating pelagic and coastal MPAs into large-scale ecosystem-wide management, *Aquatic Conserv.: Mar. Freshw. Ecosyst.*, *23*, 179–182.
- ²⁷Guizien, K., T. Brochier, J.-C. Duchêne, B.-S. Koh, and P. Marsaleix (2012), Dispersal of *Owenia fusiformis* larvae by wind-driven currents: turbulence, swimming behaviour and mortality in a three-dimensional stochastic model, *Mar. Ecol. Prog. Ser.*, *311*, 47–66.
- ²⁸Hamilton, S., J. Caselle, D. Malone, and M. Carr (2010), Incorporating biogeography into evaluations of the Channel Islands marine reserve network, *P. Natl. Acad. Sci. USA*, *107*, 18,272–18,277.
- ²⁹Hernandez-Carrasco, I., C. López, E. Hernández-García, and A. Turiel (2011), How reliable are finite-size lyapunov exponents for the assessment of ocean dynamics?, *Ocean Model.*, *36*(4), 208–218.
- ³⁰Kaplan, D., E. Chassot, A. Gruss, and A. Fonteneau (2010), Pelagic MPAs: the devil is in the details, *Trends Ecol. Evol.*, *25*, 62–63.
- ³¹Kaplan, D., S. Planes, C. Fauvelot, T. Brochier, C. Lett, N. Bodin, F. Le-Loch, Y. Tremblay, and J.-Y. Georges (2010), New tools for the spatial management of living marine resources, *Curr. Opin. Environ. Sust.*, *2*, 88–93.
- ³²Kool, J., A. Moilanen, and E. Treml (2013), Population connectivity: recent advances and new perspectives, *Landscape Ecol.*, *28*, 165–185.
- ³³Kourafalou, V., and K. Barbopoulos (2003), High resolution simulations on the North Aegean Sea seasonal circulation, *Ann. Geophys.*, *21*, 251–265.
- ³⁴Lagabrielle, E., et al. (2012), The status of Marine Protected Areas in the Mediterranean Sea, *Tech. rep.*, MEDPAN Collection, CAR/ASP.
- ³⁵Lancichinetti, A., and S. Fortunato (2009), Community detection algorithms: A comparative analysis., *Phys. Rev. E*, *80*, 056,117.
- ³⁶Lester, S., B. Halpern, K. Grorud-Colvert, J. Lubchenco, B. Ruttenberg, S. Gaines, S. Airamé, and R. R. Warner

- (2009), Biological effects within no-take marine reserves: a global synthesis, *Mar. Ecol. Prog. Ser.*, 384, 33–46.
- ³⁷Longhurst, A. R. (2006), *Ecological Geography of the Sea*, 560 pp. pp., Academic Press.
- ³⁸Macpherson, E., and N. Raventos (2006), Relationship between pelagic larval duration and geographic distribution of Mediterranean littoral fishes, *Mar. Ecol. Prog. Ser.*, 327, 257–265.
- ³⁹Madec, G., et al. (2008), Nemo ocean engine., *Tech. rep.*, Note du Pole de Modélisation, Institut Pierre-Simon Laplace (IPSL).
- ⁴⁰Mancho, A., E. Hernandez-Garcia, D. Small, S. Wiggins, and V. Fernandez (2008), Lagrangian transport through an ocean front in the north-western Mediterranean sea, *J. Phys. Ocean.*, 38, 1222–1237.
- ⁴¹Martin, A. (2000), On filament width in oceanic plankton distributions, *J. Plankton Res.*, 22(3), 597–602.
- ⁴²Millot, C., and I. Taupier-Letage (2005), Circulation in the Mediterranean Sea, in *The Mediterranean Sea, Handbook of Env. Chem.*, vol. 5K, edited by A. Salot, pp. 29–66, Springer Berlin Heidelberg.
- ⁴³Moffitt, E. A., J. W. White, and L. W. Botsford (2011), The utility and limitations of size and spacing guidelines for designing Marine Protected Area networks, *Biol. Conserv.*, 144, 306–318.
- ⁴⁴Newman, M. E. J. (2010), *Networks: An Introduction.*, Oxford Univ. Press USA.
- ⁴⁵Nilsson-Jacobi, M., C. André, K. Doos, and P. R. Jonsson (2012), Identification of subpopulations from connectivity matrices, *Ecog.*, 35, 1004–1016.
- ⁴⁶Oddo, P., M. Adani, N. Pinardi, C. Fratianni, M. Tonani, and D. Pettenuzzo (2009), A nested Atlantic-Mediterranean sea general circulation model for operational forecasting, *Ocean Sci.*, 5(4), 461–473.
- ⁴⁷Okubo, A. (1971), Ocean diffusion diagrams, *Deep Sea Res.*, 18, 789–802.
- ⁴⁸Pala, C. (2013), Giant marine reserves pose vast challenges, *Science*, 339(6120), 640–641.
- ⁴⁹Pelc, R. A., R. R. Warner, S. D. Gaines, and C. B. Paris (2010), Detecting larval export from marine reserves, *P. Natl. Acad. Sci. USA*, 107(43), 18,266–18,271.
- ⁵⁰Pineda, J., J. Hare, and S. Sponaugle (2007), Larval transport and dispersal in the coastal ocean and consequences for population connectivity, *Oceanog.*, 20(3), 22–39.
- ⁵¹Pikitch, E., et al. (2004), Ecology: ecosystem-based fishery management, *Science*, 305, 346–347.
- ⁵²Poulos, S., P. Drakopoulos, and M. Collins (1997), Seasonal variability in sea surface oceanographic conditions in the Aegean sea (eastern Mediterranean): an overview, *J. Mar. Syst.*, 13, 225–244.
- ⁵³Rosvall, M., and C. T. Bergstrom (2008), Maps of random walks on complex networks reveal community structure, *P. Natl. Acad. Sci. USA*, 105(4), 1118–1123.
- ⁵⁴Sayol, J., A. Orfila, G. Simarro, D. Conti, L. Renault, and A. Molcard (2014), A lagrangian model for tracking surface spills and SaR operations in the ocean, *Environ. Modell. Softw.*, 52, 74–82.
- ⁵⁵Shanks, A. L. (2009), Pelagic Larval Duration and dispersal distance revisited, *Biol. Bull.*, 216, 373–385.
- ⁵⁶Siegel, D. A., S. Mitarai, C. J. Costello, S. D. Gaines, B. E. Kendall, R. R. Warner, and K. B. Winters (2008), The stochastic nature of larval connectivity among nearshore marine populations, *P. Natl. Acad. Sci. USA*, 105(26), 8974–8979.
- ⁵⁷Thomas, C. J., J. Lambrechts, E. Wolanski, V. Traag, V. D. Blondel, E. Deleersnijder, and E. Hanert (2014), Numerical modelling and graph theory tools to study ecological connectivity in the Great Barrier Reef., *Ecol. Modell.*, 272, 160–174.
- ⁵⁸Tonani, M., et al. (2008), The mediterranean ocean forecasting system, coastal to global operational oceanography: Achievements and challenges, in *Proceedings of the Fifth International Conference on EuroGOOS*, edited by H. Dahlin, M. J. Bell, N. C. Fleming, and S. Pietersson, 28, EuroGOOS Publication, Sweden.
- ⁵⁹Treml, E., J. Roberts, Y. Chao, P. N. Halpin, H. Possingham, and C. Riginos (2012), Reproductive output and duration of the pelagic larval stage determine seascape-wide connectivity of marine populations, *Integr. Comp. Biol.*, 52(4), 525–537.
- ⁶⁰Vaz, A. C., K. J. Richards, Y. Jia, and C. B. Paris (2013), Mesoscale flow variability and its impact on connectivity for the island of hawaii, *Geophys. Res. Lett.*, 40, 332–337.
- ⁶¹Zulliger, D. E., S. Tanner, M. Ruch, and G. Ribi (2009), Genetic structure of the high dispersal Atlanto-Mediterranean sea star *Astropecten aranciatus* revealed by mitochondrial DNA sequences and microsatellite loci, *Mar. Biol.*, 156, 597–610.